

DEVELOPING A TWO-COLOUR ALL-FIBRE BALANCED OPTICAL CROSS-CORRELATOR FOR SUB-FEMTOSECOND SYNCHRONISATION*

J. Christie^{†1}, L. Corner¹, The University of Liverpool, Liverpool, UK
 J. R. Henderson¹, E. W. Snedden¹, ASTeC, STFC Daresbury Laboratory, UK
¹also at The Cockcroft Institute, Daresbury, UK

Abstract

Femtosecond synchronisation between an optical master oscillator (OMO) that provides facility-wide timing pulses and an external experiment laser is needed to achieve the few-fs resolution required for accelerator experiments such as pump-probe spectroscopy. This can be achieved with a balanced optical cross-correlator (BOXC), which determines the timing delay between two laser pulses via the generation of sum-frequency radiation in a nonlinear crystal.

In this paper, a design for a two-colour fibre-coupled BOXC using waveguided periodically-poled lithium niobate (PPLN) crystals is presented. An all-fibre two-colour BOXC is highly desirable as it would be more robust against environment fluctuations, easier to implement, and can achieve greater synchronisation performance compared to free-space coupled BOXCs that are currently used in accelerator facilities. This proposed design is twice as sensitive to relative timing changes between laser pulses than current free-space two-colour BOXCs, with the potential of achieving 5 - 10 times greater sensitivity. This could allow for sub-fs synchronisation between an OMO and an external experiment laser of different wavelength.

INTRODUCTION

In modern accelerator and free-electron laser (FEL) facilities, ultra-precise timing distribution systems are playing an increasingly important role. Several FELs and accelerators have implemented femtosecond timing distribution systems, consisting of a low-noise mode-locked laser synchronised to a radio frequency master oscillator (RF MO) [1, 2]. Pulses from the laser, known as the optical master oscillator (OMO), are distributed throughout the accelerator facility via stabilised fibre links which counteract optical path length fluctuations due to changes in temperature and humidity. This allows for the distribution of optical pulses with sub-femtosecond stability over kilometre-long accelerator facilities [1, 3].

To take advantage of the stability of the OMO, a suitable method of phase-locking the accelerator subsystems to the OMO pulses is required. Of particular importance is the synchronisation between the OMO and external lasers, as few-femtosecond stability is required for high temporal resolution pump-probe experiments and for precise electron bunch injection into the accelerator [4, 5]. Electrical phase-locking methods are limited to synchronisations of around 100 fs whilst also having poor long-term stability, making them

unsuitable for current accelerators [6]. To achieve the required synchronisation, an all-optical phase-locking method known as the balanced optical cross-correlator (BOXC) is used. The BOXC utilises a nonlinear crystal to determine the relative timing delay between two laser pulses from the intensity of the generated sum-frequency radiation, allowing for synchronisation of less than 10 fs [7, 8]. However, the vast majority of BOXCs in use are free-space coupled, which limits the achievable long-term stability and sensitivity due to environmental fluctuations causing the free-space optics to become misaligned over time. Although this is acceptable for current FELs and accelerators, future attosecond X-ray FELs (XFELs) will require sub-femtosecond resolution to fully exploit the short pulse durations in pump-probe experiments [9].

These issues could be addressed by a fibre-coupled BOXC, where the laser pulses travel through optical fibres to interact in a fibre-coupled nonlinear crystal. This significantly reduces the number of free-space components, improving long-term stability and synchronisation performance. Although a fibre-coupled BOXC has been demonstrated for laser pulses of the same wavelength [10, 11], a two-colour fibre-coupled BOXC has not yet been demonstrated to the best of our knowledge. Such a device would be necessary for sub-fs synchronisation between the OMO and an external laser of different wavelength, which would open many possibilities for the next generation of XFELs and linear accelerators. This paper will focus on our design of a two-colour fibre-coupled BOXC and measurements of its sensitivity, with the aim of implementing it into the synchronisation system for the Compact Linear Accelerator for Research and Applications (CLARA) located at Daresbury Laboratory [12].

PRINCIPLE OF OPERATION

The layout of the two-colour fibre-coupled BOXC is shown in Fig. 1. The BOXC is required to phase-lock a Ti:Sapphire mode-locked laser system (Micra-5), producing 50 fs long pulses at 800 nm with a bandwidth of 50 nm, to the Er:Yb OMO (Origami-15) which produces longer 200 fs pulses at 1560 nm with a bandwidth of 10 nm. To achieve this, two periodically-poled lithium niobate (PPLN) waveguides from HC Photonics [13] are used to generate the two sum-frequency pulses needed for the cross correlation. Such crystals have an effective nonlinear coefficient of $d_{eff} = 16.1 \text{ pm/V}$, around 5 times greater than that of BBO [14, 15]. The implemented waveguide reduces laser pulse diffraction as the pulses propagate through the crystal, al-

* Work supported by STFC grant no. ST/V001612/1

† Jonathan.Christie@liverpool.ac.uk

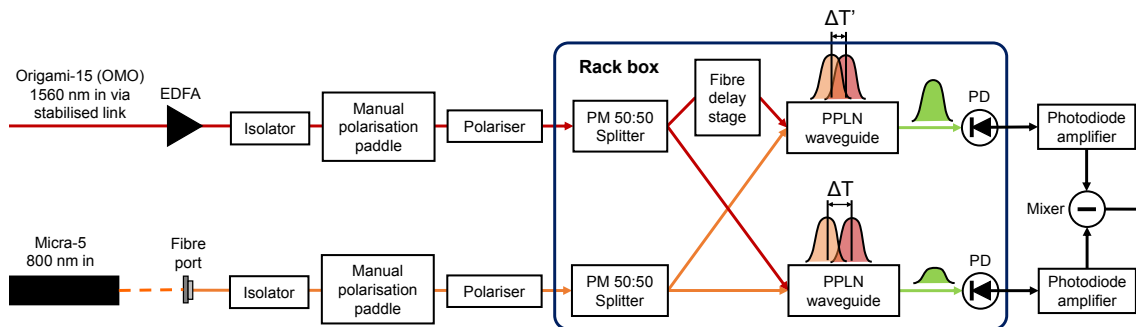


Figure 1: Layout of the two-colour fibre-coupled BOXC being developed at CLARA. The fibre delay stage increases the optical path length of one of the 1560 nm pulse components (red), resulting in the pairs of 1560 nm and 800 nm (orange) pulses having different temporal overlaps at the entrance of the two PPLN waveguides. The generated sum-frequency pulses (green) will then have different intensities, and the difference in the voltage signal from the sum-frequency pulses is proportional to the timing delay of the two input pulses.

lowing for longer interaction lengths, greater laser intensity, and thus increased sum-frequency conversion efficiency.

1560 nm pulses from the OMO are transported to the BOXC via a stabilised fibre link. The pulses are then amplified to 10 dBm by the erbium-doped fibre amplifier (EDFA). 800 nm pulses from the Micra-5 are coupled into single-mode optical fibre using a FibrePort. Both wavelengths travel to separate fibre polarisation paddles and polarisers to ensure they have the correct polarisation for the PPLN waveguides. After the paddles, polarisation-maintaining (PM) fibre is used to prevent polarisation changes within the optical fibre. The pulses then travel to PM 50:50 fibre splitters, where the wavelength components are coupled into separate PPLN waveguides such that each waveguide has a 1560 nm and 800 nm pulse. To generate the BOXC signal, one of the 1560 nm pulse components is coupled into a fibre delay stage, which increases the optical path length such that there is a fixed difference in pulse arrival time D between the two 1560 nm components. Thus, at the inputs of the PPLN waveguides, the sets of pulses have different temporal overlaps ΔT and $\Delta T' = \Delta T - D$, resulting in different amounts of sum-frequency radiation being generated by each waveguide. The sum-frequency pulses are measured by identical photodetectors and the difference in the two voltage signals is taken. This provides a balanced measurement that is insensitive to amplitude fluctuations in the initial pulses. The resulting signal is linearly proportional to the pulse time delay about the zero-crossing point, allowing for the detection of fluctuations in pulse arrival time much shorter than the pulse duration. The signal can then be used to adjust the cavity length and hence repetition rate of the 800 nm laser, with the aim of keeping the voltage difference signal locked to the zero-crossing point, resulting in the phase-locking of the two lasers to within a few femtoseconds.

EXPERIMENT SETUP

The experiment setup for generating the BOXC calibration curve is shown in Fig. 2. The OMO (Origami-15) is locked to the RF MO which operates at a frequency of

$f_{RF} = 2998.5$ MHz. The OMO then produces 1560 ± 10 nm pulses at a repetition rate of $f_{1560} = f_{RF}/12 = 249.875$ MHz. The 800 nm laser is locked to a signal generator producing an RF signal at frequency $f_{800} = (f_{1560}/3) + \delta f$, where δf is much smaller than the laser repetition rates. As the laser repetition rates are not exact multiples of each other, the temporal overlaps of the 800 nm and 1560 nm pulse trains will slowly vary in time at a fixed rate, thus scanning over the entire width of the 1560 nm pulse and generating multiple sum-frequency pulses. This generates the BOXC signal V_{BOXC} , which is recorded using an oscilloscope. The time recorded by the oscilloscope can then be converted to the relative time delay between the two pulses by the scan rate factor,

$$SR = \frac{\delta f}{f_{800}}. \quad (1)$$

For this experiment, the frequency offset is set to be $\delta f = 4.42$ Hz, giving a scan rate of $SR = 0.053$ ps/μs. At the input ports of the waveguide not connected to the fibre delay stage, the average 800 nm and 1560 nm powers are 2.82 mW and 1.63 mW respectively, and the temperature of the waveguide is set to 31.0°C. For the waveguide connected to the fibre delay stage, the average 800 nm and 1560 nm powers are 6.67 mW and 1.68 mW respectively, and the waveguide temperature is set to 40.3°C. Due to minute differences in manufacturing, the waveguides are set to different temperatures determined through testing by the waveguide manufacturer

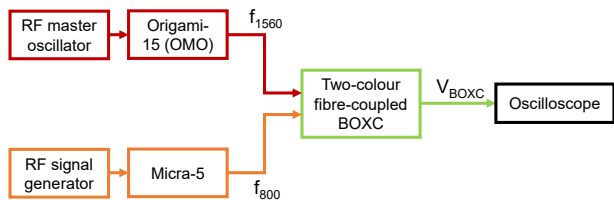


Figure 2: Experiment setup for measuring the sensitivity of the two-colour fibre-coupled BOXC.

in order to achieve maximum sum-frequency conversion. The laser pulse durations at the waveguide inputs are estimated to be approximately 1.5 ps and 1.0 ps for the 800 nm and 1560 nm pulses respectively due to dispersive broadening. To reduce the background signal from the 800 nm pulses passing through the waveguides, a wavelength-division multiplexer (WDM) is connected to each waveguide output to separate the 528.8 nm sum-frequency pulses and the 800 nm pulses. The sum-frequency signal is detected by a slow photodetector (DET025AFC_M, Thorlabs) with responsivity $\alpha = 0.18 \text{ A/W}$ at 528.8 nm before being amplified by a photodiode amplifier (PDA200C, Thorlabs) with the gain set to $G = 10^5 \text{ V/A}$. This stops us from being able to observe individual sum-frequency pulses but helps reduce overall noise. The oscilloscope then records the two voltage signals and subtracts one from the other to generate the BOXC calibration curve, and the oscilloscope time scale is converted to real time by multiplying the time scale by the scan rate SR .

RESULTS AND DISCUSSION

Plots of the sum-frequency signal from both waveguides and the BOXC calibration curve are given in Fig. 3. From the gradient of the BOXC curve about the point where $V = 0$, the sensitivity is found to be 0.971 mV/fs. Accounting for differences in transimpedance gain and photodetector responsivity, the sensitivity is twice that of comparable free-space two-colour BOXCs [8].

To determine the effect that changing parameters such as the laser power or laser pulse duration would have on the BOXC signal, the theoretical BOXC sensitivity can be calculated through numerical integration of the wave equation for the sum-frequency pulses over the length of the waveguides [10]. As shown in Fig. 3, reducing the pulse durations of the 800 nm and 1560 nm lasers by a factor of 2 gives a theoretical sensitivity of 4.2 mV/fs. The 5 times greater sensitivity compared to our current results is due to the increased pulse intensity and the sharper sum-frequency voltage signals. Further optimisation could allow for sensitivities 10 times greater than free-space two-colour BOXCs, which would be an important step towards sub-fs synchronisation.

CONCLUSION

A two-colour fibre-coupled balanced optical cross-correlator has been demonstrated for the first time to the best of our knowledge. A sensitivity of 0.971 mV/fs was achieved, which is greater than comparable free-space two-colour BOXCs after accounting for transimpedance gain and photodetector responsivity. Further investigation into improving the sensitivity through reducing pulse duration, increasing laser power, and optimising other factors such as waveguide temperature and responsivity will be made before using the fibre-coupled BOXC to phase-lock the 800 nm laser to the 1560 nm optical master oscillator. Once phase-locking is achieved, the long-term timing stability of the fibre-coupled BOXC will be compared against a free-space

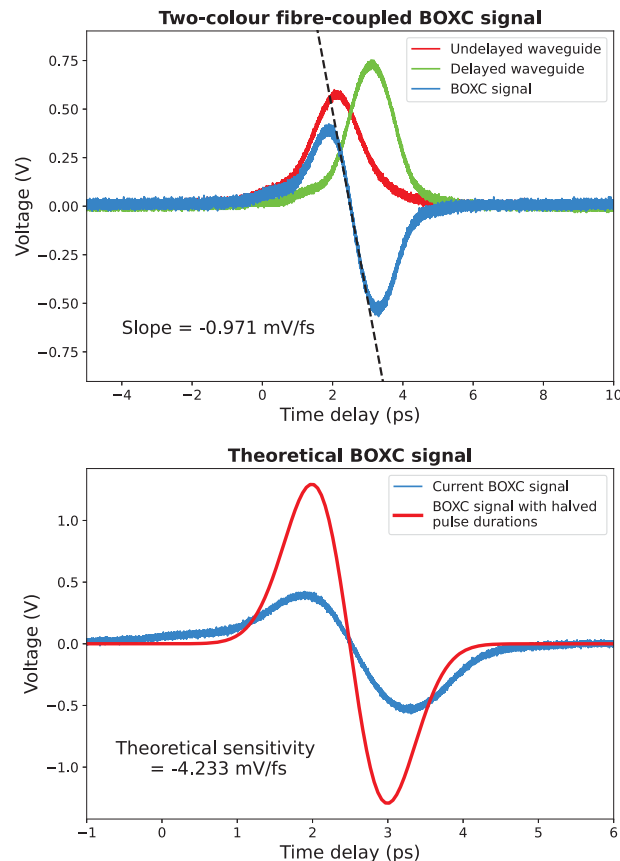


Figure 3: (top) Voltage signals from the undelayed waveguide (red) and the waveguide coupled to the fibre delay stage (green), and the BOXC calibration curve (blue) corresponding to the difference between those two signals. (bottom) Comparison between current BOXC signal (blue) and theoretical BOXC signal (red) after halving the 800 nm and 1560 nm pulse durations.

BOXC to determine the impact of using fibre-coupled components.

Future work will involve packaging the fibre-coupled BOXC into a single rack box that can be easily stored in an environmentally-controlled area by minimising the number of fibre components and the amount of optical fibre used, which will additionally improve the sensitivity. This would allow for the fibre-coupled BOXC to be implemented into the synchronisation system for the Full Energy Beam Exploitation (FEBE) upgrade to CLARA, potentially making sub-femtosecond temporal resolution on pump-probe and novel acceleration experiments possible at Daresbury Laboratory.

REFERENCES

[1] M. Xin, K. Şafak, and F. X. Kärtner, “Ultra-precise timing and synchronization for large-scale scientific instruments,” *Optica*, vol. 5, no. 12, p. 1564, 2018.
doi:10.1364/optica.5.001564

[2] S. Schulz *et al.*, “Few-femtosecond facility-wide synchronization of the European XFEL,” in *Proc. FEL’19*, Hamburg, Germany, 2019, pp. 318–321.
doi:10.18429/JACoW-FEL2019-WEBO4

[3] A. J. Benedick, J. G. Fujimoto, and F. X. Kärtner, “Optical flywheels with attosecond jitter,” *Nature Photonics*, vol. 6, no. 2, pp. 97–100, 2012.
doi:10.1038/nphoton.2011.326

[4] P. Vester *et al.*, “Ultrafast structural dynamics of photo-reactions observed by time-resolved x-ray cross-correlation analysis,” *Structural Dynamics*, vol. 6, no. 2, p. 024301, 2019. doi:10.1063/1.5086374

[5] A. J. Reitsma, R. A. Cairns, R. Bingham, and D. A. Jaroszynski, “Efficiency and energy spread in laser-wakefield acceleration,” *Physical Review Letters*, vol. 94, no. 8, pp. 1–4, 2005.
doi:10.1103/PhysRevLett.94.085004

[6] J. M. Głownia *et al.*, “Time-resolved pump-probe experiments at the LCLS,” *Optics Express*, vol. 18, no. 17, p. 17620, 2010. doi:10.1364/oe.18.017620

[7] S. Schulz *et al.*, “Femtosecond all-optical synchronization of an X-ray free-electron laser,” *Nature Communications*, vol. 6, no. 1, p. 5938, 2015. doi:10.1038/ncomms6938

[8] C. L. Li, L. Feng, B. Liu, J. G. Wang, X. T. Wang, and W. Y. Zhang, “Two Color Balanced Optical Cross Correlator to Synchronize Distributed Lasers for SHINE Project,” in *Proc. IBIC’21*, Pohang, Korea, 2021, pp. 370–372.
doi:10.18429/JACoW-IBIC2021-WEPP05

[9] H.-S. Kang and I. S. Ko, “Attosecond XFEL for pump–probe experiments,” *Nature Photonics*, vol. 14, no. 1, pp. 7–8, 2020.
doi:10.1038/s41566-019-0570-8

[10] P. T. Callahan, K. Safak, P. Battle, T. D. Roberts, and F. X. Kärtner, “Fiber-coupled balanced optical cross-correlator using PPKTP waveguides,” *Opt. Express*, vol. 22, no. 8, pp. 9749–9758, 2014.
doi:10.1364/OE.22.009749

[11] K. Safak *et al.*, “Extreme-timing-resolution with waveguide-based balanced optical cross-correlators,” in *Conference on Lasers and Electro-Optics*, 2022, STh5N.3.
doi:10.1364/CLEO_SI.2022.STh5N.3

[12] P. McIntosh *et al.*, “The VELA and CLARA Test Facilities at Daresbury Laboratory,” in *Proc. of LINAC’16*, East Lansing, MI, USA, 2017, pp. 734–739.
doi:10.18429/JACoW-LINAC2016-TH3A03

[13] HC Photonics, *HC Photonics Corp.* <https://www.hcphotonics.com/>, Accessed: 2023-04-03, 2017.

[14] V. G. Dimitriev, G. G. Gurzadyan, and D. N. Nikogosyan, “Handbook of nonlinear optical crystals,” eng, in *Handbook of nonlinear optical crystals*, 3rd, rev. 1999, pp. 96–103.

[15] HC Photonics, *PPLN Guide: Overview*, <https://www.hcphotonics.com/ppln-guide-overview>, Accessed: 2023-04-03, 2017.